

Study of $B_c^- \rightarrow J/\psi\pi^-, \eta_c\pi^-$ Decays with QCD Factorization

Junfeng Sun,¹ Guifeng Xue,¹ Yueling Yang,¹ Gongru Lu,¹ and Dongsheng Du²

¹*College of Physics and Information Engineering,
Henan Normal University, Xinxiang 453007, China**

²*Institute of High Energy Physics, Chinese Academy of Sciences,
P.O.Box 918(4), Beijing 100049, China*

Abstract

The $B_c \rightarrow J/\psi\pi, \eta_c\pi$ decays are studied in the scheme of the QCD factorization approach. The branching ratios are calculated with the asymptotic distribution amplitude of the pion. The charm quark mass effect is considered. We find that the mass effect on the branching ratios is small.

PACS numbers: 12.38.Bx 12.39.St 13.25.Hw

arXiv:0710.0031v2 [hep-ph] 19 Apr 2008

*Mailing address

I. INTRODUCTION

The B_c meson is the ground state of the b - c system. It is a quarkonium state consisting of heavy quarks with different flavours, and it lies below the threshold of the BD mesons. It cannot annihilate into gluons, so it can only decay weakly. The B_c system offers a new ideal place for studying the weak decay mechanism of heavy flavors and testing of the quark-flavour-mixing sector of the Standard Model. The discovery of the B_c meson by the CDF [1] has demonstrated the possibility for the experimental investigation of this system.

B_c mesons are too massive to produce at e^+e^- colliders operating near $\Upsilon(4S)$, such as the “ B factories” at SLAC and KEK. They can be produced in significant numbers in hadron colliders. The Large Hadron Collider (LHC) is scheduled to run in 2008. Due to its high collision energy and high luminosity, the expected large production rates at the LHC will allow for precision measurements of B_c properties. The B -physics, including the physics potential of the B_c system, could be fully exploited at the LHC. Measurements of heavy quarkonia at the LHC will be valuable for a deep understanding of the production and decay mechanisms of the corresponding quarkonia involved.

The B_c meson has very rich weak decay channels which can be divided into three classes: (1) the b quark decay ($b \rightarrow c, u$) with c quark as a spectator, (2) the c quark decay ($c \rightarrow s, d$) with b quark as a spectator, and (3) the annihilation channel. Clearly, we can study the two heavy flavors b and c simultaneously with B_c meson. For the case of Class (1), the precision determination of the Cabibbo-Kobayashi-Maskawa (CKM) [2] matrix elements of $|V_{cb}|$ and $|V_{ub}|$ are interesting, where determinations of $|V_{ub}|$ based on inclusive and exclusive channels have an uncertainty of 8% and 17% at present, respectively [3]. For the case of Class (2), although the heavy B_s (or B_u, B_d) in the final state has a considerable effect in reducing the phase space for c quark decay, the CKM matrix elements $|V_{cb}| \ll |V_{cs}|$ is in favor of the c quark decay greatly. For the case of Class (3), the B_c weak annihilation decays are CKM enhanced by $|V_{cb}/V_{ub}|^2 \sim 10^2$ as compared to B_u annihilation decays. All the three classes listed above are interesting.

The B_c meson decay has been widely studied in the literature due to some of its outstanding features. The earlier nonleptonic decays of B_c meson has been studied in [4, 5, 6, 7, 8, 9, 10, 11, 12, 13, 14, 15, 16, 17, 18, 19]. The theoretical status of the B_c meson was reviewed in [19]. In this paper, we will concentrate on the $B_c \rightarrow J/\psi\pi, \eta_c\pi$

decays in Class (1) with QCD factorization approach. Let us outline a few reasons below.

- The LHCb detector has a high trigger performance, good resolution for interaction vertex, excellent particle identification for charged particles. So all final-state particles are detectable for the $B_c \rightarrow J/\psi\pi, \eta_c\pi$ decays. In practice, the most constructive information is to extract a signal of J/ψ (or η_c) from the cascade decays [20]. Especially, compared with the semi-leptonic decays where the neutrino momentum is not detected directly, the LHC can provide a clean signature for $B_c \rightarrow J/\psi\pi, \eta_c\pi$ due to the narrow-peak of J/ψ (or η_c) and the good identification of the charged pion. It is estimated that one could expect around 5×10^{10} B_c events per year at LHC, so ATLAS would be able to record about 5600 events of $B_c \rightarrow J/\psi\pi$ in one year [19]. Better signal-to-background ratios and larger yields make $B_c \rightarrow J/\psi\pi, \eta_c\pi$ decay modes to be the most prospective channels for measurements.
- The final states of $B_c \rightarrow J/\psi\pi, \eta_c\pi$ decays have large momentum compared with the Class (2) decays (e.g. $B_c \rightarrow B + X$ decays), so the final state interactions can be neglected among the energetic particles. One can effectively factorize the hard and soft amplitudes. Further more, the behavior of interaction vertices modified by hard gluon corrections at large recoil can be calculated reliably with perturbation theory.
- For the exploration of CP violation, the key processes are nonleptonic B decays. The theoretical challenge is the calculation of the hadronic transition matrix elements $\langle f|\hat{Q}_i|B\rangle$, where \hat{Q}_i is the local four quark operator. Recently, several attractive methods have been proposed to study the “nonfactorizable” effects in hadronic matrix elements, such as the QCD factorization (QCDF) [21], perturbative QCD method [22, 23, 24], soft collinear effective theory [25, 26]. The nonleptonic two-body B_u, B_d, B_s decays have been studied in detail, for example, in Refs. [27, 28, 29, 30, 31, 32, 33, 34, 35, 36, 37, 38, 39]. It is found that with appropriate parameters, most of the theoretical predictions are in agreement with the present experimental data. With the accumulation of data, the Standard Model can be tested in more detail. The potential B_c decay modes permit us to over-constrain the angles and sides of the *unitarity triangle* of the CKM matrix. The $B_c \rightarrow J/\psi\pi, \eta_c\pi$ decays are a_1 dominant within the framework of Operator Product Expansion (OPE). They do not have pollution from penguins and annihilation diagrams. Moreover, the coefficient of

a_1 can be well determined compared with other coefficients. So these decays could be used for determination of the CKM matrix element $|V_{cb}|$.

- In the limit of infinitely heavy quark masses, the HQET Lagrangians possess spin symmetry. The B_c decays to $J/\psi, \eta_c$ involve the heavy spectator quark. The spectator enters the heavy hadron in the final states with no hard gluon rescattering, because spin symmetry works only at recoil momenta close to zero. The transition form factors should be nonperturbative hadronic quantities. It is expected that the quark-gluon sea is suppressed for B_c mesons and that the calculation of factorization can be applied for non-leptonic B_c decay. Thus the important parameter is the factor a_1 which depends on the normalization scale [19]. The authors of [4, 5, 6, 7, 8, 9, 10, 11, 12, 13, 14, 15, 16, 17, 18] have much concern for hadron transition form factors whose dependence on the momentum transfer is not significant within the physical phase space [19], rather than the factor a_1 . Moreover, for the exploration of CP violation in B_c decays, it needs to know the strong phases in addition to weak phases. While only the real value of the factor a_1 at the fixed point is used in the previous work [4, 5, 6, 7, 8, 9, 10, 11, 12, 13, 14, 15, 16, 17, 18]. In this paper, we will consider the radiative corrections to the hadron matrix element to compensate the renormalization scale dependence of Wilson coefficients. In addition, some information of strong phases can be obtained.

This paper is organized as follows: In section II, we discuss the theoretical framework and compute the decay amplitudes for $B_c \rightarrow J/\psi\pi, \eta_c\pi$ with the master QCD formula. The section III is devoted to the numerical results. Finally, we summarize in section IV.

II. THEORETICAL FRAMEWORK

A. The effective Hamiltonian

Using the operator product expansion and renormalization group equation, the low energy effective Hamiltonian for $B_c \rightarrow J/\psi\pi, \eta_c\pi$ decays can be written as [40]:

$$\mathcal{H}_{eff} = \frac{G_F}{\sqrt{2}} V_{cb} V_{ud}^* \{ C_1(\mu) Q_1 + C_2(\mu) Q_2 \} + \text{H.c.}, \quad (1)$$

where $V_{cb} V_{ud}^*$ is the CKM factors. The expressions of the local tree operators are

$$Q_1 = (\bar{c}_\alpha b_\alpha)_{V-A} (\bar{d}_\beta u_\beta)_{V-A} \quad Q_2 = (\bar{c}_\alpha b_\beta)_{V-A} (\bar{d}_\beta u_\alpha)_{V-A} \quad (2)$$

Note that there is no local penguin operators, thus no interference between tree and penguin operators, and no CP asymmetry for these decays. The coupling parameters $C_i(\mu)$ are Wilson coefficients which have been evaluated to the next-to-leading order (NLO). Their numerical values in the naive dimensional regularization scheme (NDR) are listed in Table I.

B. Hadronic matrix elements within the QCDF framework

For the weak decays of hadrons, the short-distance effects are well known and can be calculated with perturbation theory. However, the nonperturbative long-distance effects responsible for the hadronization from quarks to hadrons still remain obscure in several aspects. But to calculate the exclusive weak decays of the B_c meson, one needs to evaluate the hadronic matrix elements, i.e., the weak current operator sandwiched between the initial state of the B_c meson and the concerned hadronic final states, which is the most difficult theoretical work at present. Phenomenologically, these hadronic matrix elements are usually parameterized into the product of the decay constants and the transition form factors based on the naive factorization scheme (NF) [41]. However, the main defect of the rough NF approach is that the hadronic matrix elements cannot compensate the renormalization scheme- and scale- dependence of Wilson coefficients. In that sense the NF's results are unphysical. Moreover, for the exploration of CP violation, information of the strong phases is needed, but the values of both the hadronic matrix elements and the Wilson coefficients are real within NF. These indicate that “nonfactorizable” contributions from high order corrections to the hadronic matrix elements must be taken into account.

A few years ago, Beneke, Buchalla, Neubert, and Sachrajda suggested a QCDF formula to compute the hadronic matrix elements $\langle M_1 M_2 | O_i | B \rangle$ in the heavy quark limit, combining the hard scattering approach with power counting in $1/m_b$ [21]. At leading order in the heavy quark expansion, the hadronic matrix elements can be factorized into “non-factorizable” corrections dominated by hard gluon exchange and universal non-perturbative part parameterized by the physical form factors and meson's light cone distribution amplitudes. This promising method has been applied to exclusive two-body non-leptonic B_u , B_d , B_s decays [33, 34, 35]. It is found that with appropriate parameters, most of the QCDF's predictions are in agreement with the present experimental data. In this paper, we would like to apply

the QCDF approach to the case of $B_c \rightarrow J/\psi\pi$, $\eta_c\pi$ decays.

In the heavy quark limit $m_b \gg \Lambda_{QCD}$, up to power corrections of order of Λ_{QCD}/m_b , the master QCDF formula for $B_c \rightarrow \eta_c\pi$ (or $J/\psi\pi$) can be written as [21]

$$\langle \eta_c\pi | O_i | B_c \rangle = F^{B_c \rightarrow \eta_c} \int_0^1 dz H(z) \Phi_\pi(z) \quad (3)$$

Through the QCDF formula Eq.(3), the hadronic matrix elements can be separated into short-distance part [hard-scattering kernels $H(z)$] and long-distance part. At leading order of α_s , $H(z) = 1$. There is no long-distance interaction between pion and $B_c\text{-}\eta_c$ (or $B_c\text{-}J/\psi$) system, so the NF's picture is recovered. Nonperturbative effects are either suppressed by $1/m_b$ or parameterized in terms of the transition form factors $F^{B_c \rightarrow \eta_c}$ (or $F^{B_c \rightarrow J/\psi}$) and the meson's light-cone distribution amplitudes $\Phi(z)$.

C. Discussions on soft and collinear divergence cancellation at one-loop order

When we calculate the vertex corrections in the leading power of Λ_{QCD}/m_b , not only ultraviolet divergence emerges but also infrared divergence, as shown in [42]. The authors of [21] gave an explicit cancellation of soft and collinear divergences in vertex corrections for $B \rightarrow D\pi$ decays. They demonstrated that the soft divergences cancel out in Fig.1(a) and Fig.1(b), and in Fig.1(c) and Fig.1(d), respectively; the collinear divergences cancel out in Fig.1(a) and Fig.1(c), and in Fig.1(b) and Fig.1(d), respectively. For $B_c \rightarrow J/\psi\pi$, $\eta_c\pi$ decays, the soft and collinear divergence cancellations are the same as that for $B \rightarrow D\pi$ decays in [21], because they are all $b \rightarrow c$ transition. Here, we will consider the non-zero mass of c quark, and give an explicit calculation of the Feynman diagrams Fig.1(a)-(d) to show the cancellation of the infrared divergence, as shown in [42].

The two valence quarks in pion have transverse momentum as well as longitudinal momentum. The quark and antiquark momenta in pion meson is

$$k_q = zq + \vec{k}_\perp, \quad k_{\bar{q}} = \bar{z}q - \vec{k}_\perp \quad (4)$$

where $q \sim \mathcal{O}(m_b)$ is the momentum of the emitted π meson; z and $\bar{z} \equiv 1 - z$ are the longitudinal momentum fraction of quark and anti-quark, respectively; $\vec{k}_\perp \sim \mathcal{O}(\Lambda_{QCD})$ is the transverse momentum. But in $B_c \rightarrow J/\psi\pi$, $\eta_c\pi$ decays, the pion is energetic. So the dominant contribution to the pion wave function comes from configurations where two

valence quarks are hard. The contribution from soft regions at the endpoint is believed to be suppressed in the heavy-quark limit. For our case, the quark is on-shell, and the effects proportional to \vec{k}_\perp is power suppressed.

Now we shall take into account the α_s corrections to the hadronic matrix element. After a straightforward calculation in the NDR scheme as in [42], we obtain

$$\begin{aligned}
\langle Q_2 \rangle_{(a)} &= \frac{\alpha_s C_F}{4\pi N} \langle \pi^- | (\bar{d}u)_{V-A} | 0 \rangle \langle J/\psi | (\bar{c}b)_{V-A} | B_c^- \rangle \\
&\times \left\{ - \left(\frac{m_b^2}{\mu^2} \right)^\epsilon \frac{\Gamma(1-\epsilon)}{(4\pi)^\epsilon} \left[\frac{1}{\epsilon^2} + \frac{2}{\epsilon} (\ln t_a - 1) + \ln^2 t_a + \frac{2 \ln t_a}{1-t_a} - 4 \ln t_a - 2 \text{Li}_2 \left(\frac{t_a-1}{t_a} \right) + 5 \right. \right. \\
&\quad \left. \left. + r_c \left(\frac{t_a \ln t_a}{(1-t_a)^2} + \frac{1}{1-t_a} \right) \right] \right. \\
&\quad \left. + \left(\frac{\mu^2}{m_b^2} \right)^\epsilon (4\pi)^\epsilon \Gamma(1+\epsilon) \left[\frac{1}{\epsilon} + \frac{t_a \ln t_a}{1-t_a} + 1 \right] \right\} \quad (5)
\end{aligned}$$

$$\begin{aligned}
\langle Q_2 \rangle_{(b)} &= \frac{\alpha_s C_F}{4\pi N} \langle \pi^- | (\bar{d}u)_{V-A} | 0 \rangle \langle J/\psi | (\bar{c}b)_{V-A} | B_c^- \rangle \\
&\times \left\{ + \left(\frac{m_b^2}{\mu^2} \right)^\epsilon \frac{\Gamma(1-\epsilon)}{(4\pi)^\epsilon} \left[\frac{1}{\epsilon^2} + \frac{2}{\epsilon} (\ln t_b - 1) + \ln^2 t_b + \frac{2 \ln t_b}{1-t_b} - 4 \ln t_b - 2 \text{Li}_2 \left(\frac{t_b-1}{t_b} \right) + 6 \right] \right. \\
&\quad \left. - \left(\frac{\mu^2}{m_b^2} \right)^\epsilon (4\pi)^\epsilon \Gamma(1+\epsilon) \left[\frac{4}{\epsilon} + 4 \frac{t_b \ln t_b}{1-t_b} + 11 \right] \right\} \quad (6)
\end{aligned}$$

$$\begin{aligned}
\langle Q_2 \rangle_{(c)} &= \frac{\alpha_s C_F}{4\pi N} \langle \pi^- | (\bar{d}u)_{V-A} | 0 \rangle \langle J/\psi | (\bar{c}b)_{V-A} | B_c^- \rangle \\
&\times \left\{ + \left(\frac{m_c^2}{\mu^2} \right)^\epsilon \frac{\Gamma(1-\epsilon)}{(4\pi)^\epsilon} \left[\frac{1}{\epsilon^2} + \frac{2}{\epsilon} (\ln t_c - 1) + \ln^2 t_c + \frac{2 \ln t_c}{1-t_c} - 4 \ln t_c - 2 \text{Li}_2 \left(\frac{t_c-1}{t_c} \right) + 6 \right] \right. \\
&\quad \left. - \left(\frac{\mu^2}{m_c^2} \right)^\epsilon (4\pi)^\epsilon \Gamma(1+\epsilon) \left[\frac{4}{\epsilon} + 4 \frac{t_c \ln t_c}{1-t_c} + 11 \right] \right\} \quad (7)
\end{aligned}$$

$$\begin{aligned}
\langle Q_2 \rangle_{(d)} &= \frac{\alpha_s C_F}{4\pi N} \langle \pi^- | (\bar{d}u)_{V-A} | 0 \rangle \langle J/\psi | (\bar{c}b)_{V-A} | B_c^- \rangle \\
&\times \left\{ - \left(\frac{m_c^2}{\mu^2} \right)^\epsilon \frac{\Gamma(1-\epsilon)}{(4\pi)^\epsilon} \left[\frac{1}{\epsilon^2} + \frac{2}{\epsilon} (\ln t_d - 1) + \ln^2 t_d + \frac{2 \ln t_d}{1-t_d} - 4 \ln t_d - 2 \text{Li}_2 \left(\frac{t_d-1}{t_d} \right) + 5 \right. \right. \\
&\quad \left. \left. + \frac{1}{r_c} \left(\frac{t_d \ln t_d}{(1-t_d)^2} + \frac{1}{1-t_d} \right) \right] \right. \\
&\quad \left. + \left(\frac{\mu^2}{m_c^2} \right)^\epsilon (4\pi)^\epsilon \Gamma(1+\epsilon) \left[\frac{1}{\epsilon} + \frac{t_d \ln t_d}{1-t_d} + 1 \right] \right\} \quad (8)
\end{aligned}$$

where $\epsilon \rightarrow 0^+$ for ultraviolet divergences, $\epsilon \rightarrow 0^-$ for infrared divergences, $r_c = m_c/m_b$, and

$$t_a = z(1-r_c^2) \quad (9)$$

$$t_b = \bar{z}(1-r_c^2) \quad (10)$$

$$t_c = z(1-1/r_c^2) = -t_a/r_c^2 \quad (11)$$

$$t_d = \bar{z}(1-1/r_c^2) = -t_b/r_c^2 \quad (12)$$

In Eq.(7), the term of infrared divergences can be written as

$$\begin{aligned}
& \left(\frac{m_c^2}{\mu^2}\right)^\epsilon \left[\frac{1}{\epsilon^2} + \frac{2}{\epsilon}(\ln t_c - 1) + \dots \right] \\
&= \left(\frac{m_b^2}{\mu^2}\right)^\epsilon \left(\frac{m_c^2}{m_b^2}\right)^\epsilon \left[\frac{1}{\epsilon^2} + \frac{2}{\epsilon} \left(\ln \frac{-t_a}{r_c^2} - 1 \right) + \dots \right] \\
&= \left(\frac{m_b^2}{\mu^2}\right)^\epsilon \left[\frac{1}{\epsilon^2} + \frac{2}{\epsilon}(\ln t_a - 1) - \frac{1}{\epsilon}(\ln r^2 + i 2\pi) + \dots \right]
\end{aligned} \tag{13}$$

We can treat the infrared divergences in Eq.(8) in the same way.

$$\begin{aligned}
& \left(\frac{m_c^2}{\mu^2}\right)^\epsilon \left[\frac{1}{\epsilon^2} + \frac{2}{\epsilon}(\ln t_d - 1) + \dots \right] \\
&= \left(\frac{m_b^2}{\mu^2}\right)^\epsilon \left(\frac{m_c^2}{m_b^2}\right)^\epsilon \left[\frac{1}{\epsilon^2} + \frac{2}{\epsilon} \left(\ln \frac{-t_b}{r_c^2} - 1 \right) + \dots \right] \\
&= \left(\frac{m_b^2}{\mu^2}\right)^\epsilon \left[\frac{1}{\epsilon^2} + \frac{2}{\epsilon}(\ln t_b - 1) - \frac{1}{\epsilon}(\ln r^2 + i 2\pi) + \dots \right]
\end{aligned} \tag{14}$$

So it is easy to see that the infrared divergences are cancelled in the summation of all diagrams in Fig.1 before we integrate over the momentum fraction variable z . That is to say that the decay amplitude is infrared finite in the soft region when \vec{k}_\perp is neglected. This can be understood as a technical manifestation of colour transparency.

Within the modified minimal subtraction ($\overline{\text{MS}}$) scheme, we get

$$\begin{aligned}
& \langle Q_2 \rangle_{(a)+(b)+(c)+(d)} \\
&= \frac{\alpha_s C_F}{4\pi N} \langle \pi^- | (\bar{d}u)_{V-A} | 0 \rangle \langle J/\psi | (\bar{c}b)_{V-A} | B_c^- \rangle \\
&\times \left\{ \left[\frac{t_a \ln t_a}{1-t_a} - \frac{4t_b \ln t_b}{1-t_b} + 3 \ln \left(\frac{m_b^2}{\mu^2} \right) - 9 \right] - r_c \left[\frac{t_a \ln t_a}{(1-t_a)^2} + \frac{1}{1-t_a} \right] \right. \\
&+ \left[\frac{t_d \ln t_d}{1-t_d} - \frac{4t_c \ln t_c}{1-t_c} + 3 \ln \left(\frac{m_c^2}{\mu^2} \right) - 9 \right] - \frac{1}{r_c} \left[\frac{t_d \ln t_d}{(1-t_d)^2} + \frac{1}{1-t_d} \right] \\
&\left. + 2(\ln t_a - \ln t_b) \ln r_c^2 - f(t_a) + f(t_b) + f(t_c) - f(t_d) \right\}
\end{aligned} \tag{15}$$

where

$$f(t) = \ln^2 t + \frac{2t \ln t}{1-t} - 2\text{Li}_2\left(\frac{t-1}{t}\right) \tag{16}$$

From above we found that the expressions of Eq.(15) and Eq.(16) are consistent with the result [see Eq.(80)—Eq.(85)] in the previous works [21].

With Eq.(15) and Eq.(16), we can compute the “non-factorizable” contribution of the one-gluon exchange vertex correction no matter the distribution amplitude $\phi(z)$ is symmetric or not. This is very important in principle. For instance, when kaon is ejected from b quark

decay, the contribution from the asymmetric part of kaon distribution amplitude must be taken into account, although the contributions from the asymmetric part might be very small numerically.

From the above, we can see that the “nonfactorizable” interactions connecting the $B_c \rightarrow J/\psi$ (or η_c) transition and the emitted pion are dominated by hard gluon exchange. So we may perform the \vec{k}_\perp integration over the pion wave function. We define [21]

$$\begin{aligned} \langle \pi(q) | \bar{d}_\alpha(x) u_\beta(0) | 0 \rangle &= \int \mathbf{d}z \frac{\mathbf{d}^2 \vec{k}_\perp}{16\pi^3} \frac{e^{ik_d \cdot x}}{\sqrt{2N_c}} \Psi_\pi(z, \vec{k}_\perp) [\gamma_5 \not{A}]_{\alpha\beta} \\ &= -\frac{if_\pi}{4N_c} \int \mathbf{d}z \phi_\pi(z) [\gamma_5 \not{A}]_{\alpha\beta} \end{aligned} \quad (17)$$

Assuming that the distribution amplitude $\phi_\pi(z)$ is symmetric, i.e. $\phi_\pi(z) = \phi_\pi(\bar{z})$, then Eq.(15) can be simplified as follows:

$$\begin{aligned} &\langle Q_2 \rangle_{(a)+(b)+(c)+(d)} \\ &= \frac{\alpha_s C_F}{4\pi N} \langle \pi^- | (\bar{d}u)_{V-A} | 0 \rangle \langle J/\psi | (\bar{c}b)_{V-A} | B_c^- \rangle \\ &\times \left\{ 3 \left[\ln\left(\frac{m_b^2}{\mu^2}\right) + \ln\left(\frac{m_c^2}{\mu^2}\right) - \frac{t_a \ln t_a}{1-t_a} - \frac{t_d \ln t_d}{1-t_d} - 6 \right] \right. \\ &\quad \left. - \left[r_c \left(\frac{t_a \ln t_a}{(1-t_a)^2} + \frac{1}{1-t_a} \right) + \frac{1}{r_c} \left(\frac{t_d \ln t_d}{(1-t_d)^2} + \frac{1}{1-t_d} \right) \right] \right\} \end{aligned} \quad (18)$$

Now we present the results of the coefficients a_1 for the case of $B_c \rightarrow J/\psi\pi$, $\eta_c\pi$ decays. Similar results hold for all Class (1) (a_1 -dominant) $b \rightarrow cqq'$ (where q and q' are light quarks) transition processes.

$$a_1 = C_1^{(\text{NLO})} + \frac{C_2^{(\text{NLO})}}{N_c} + \frac{\alpha_s C_F}{4\pi N_c} C_2^{(\text{LO})} V \quad (19)$$

The vertex corrections V are given as follows [note: here $\phi(z) = \phi(\bar{z})$ is assumed]:

- for the $m_c \neq 0$ case

$$V = 3 \ln\left(\frac{m_b^2}{\mu^2}\right) + 3 \ln\left(\frac{m_c^2}{\mu^2}\right) - 18 - \int \mathbf{d}z \phi(z) H_1(z) \quad (20)$$

where

$$H_1(z) = \frac{3t_a \ln t_a}{1-t_a} + \frac{3t_d \ln t_d}{1-t_d} + r_c \left(\frac{t_a \ln t_a}{(1-t_a)^2} + \frac{1}{1-t_a} \right) + \frac{1}{r_c} \left(\frac{t_d \ln t_d}{(1-t_d)^2} + \frac{1}{1-t_d} \right) \quad (21)$$

- for the $m_c = 0$ case [32, 42]

$$V = 3 \left\{ 2 \ln\left(\frac{m_b^2}{\mu^2}\right) - 6 - i\pi + \int \mathbf{d}z \phi(z) \frac{\bar{z} - z}{1-z} \ln z \right\} \quad (22)$$

D. The renormalization scale dependence

From the expressions of the coefficient a_1 in Eq.(19), apparently, the renormalization scale dependence of the hadronic matrix element is recovered, i.e. $\langle Q_2(\mu) \rangle = g(\mu)\langle Q_2 \rangle$. We expect that the recovered scale dependence from $g(\mu)$ can cancel the scale dependence of the Wilson coefficients $C_i(\mu)$, at least in part.

With the renormalization group equations for the Wilson coefficients at leading order (LO) approximation [40]

$$\frac{\mathbf{d}}{\mathbf{d}\ln\mu} \begin{pmatrix} C_1(\mu) \\ C_2(\mu) \end{pmatrix} = \frac{\alpha_s}{4\pi} \gamma_s^{(0)T} \begin{pmatrix} C_1(\mu) \\ C_2(\mu) \end{pmatrix} \quad (23)$$

where the matrix of the LO anomalous dimensions $\gamma_s^{(0)}$ is [40]

$$\gamma_s^{(0)} = \begin{pmatrix} -6/N_c & 6 \\ 6 & -6/N_c \end{pmatrix} \quad (24)$$

It is easy to find that when the contributions from higher order of α_s are neglected, we have

$$\frac{\mathbf{d}}{\mathbf{d}\ln\mu} a_1 = \frac{\mathbf{d}}{\mathbf{d}\ln\mu} \left(C_1(\mu) + \frac{C_2(\mu)}{N_c} \right) + \frac{\alpha_s}{4\pi} \frac{C_2(\mu)}{N_c} C_F \frac{\mathbf{d}}{\mathbf{d}\ln\mu} V = 0 \quad (25)$$

Eq.(25) just show that the coefficient a_1 is no longer scale-dependent at the order of α_s . Of course, a_1 is still scale-dependent beyond the order of α_s corrections. This can be seen from both Fig.2 and the numbers in Table I. In principle, we have to include contributions of all higher order of α_s corrections to cancel the remaining scale dependence of a_1 .

E. Gauge dependence

To demonstrate the gauge dependence, firstly we would like to write down the one-gluon exchange contribution to $B_c \rightarrow J/\psi\pi$ matrix element of the operator Q_2 . Following the expression of Eq.(55)—Eq.(57) in [21], we have

$$\langle Q_2 \rangle_{\text{Fig.1}} = -i \frac{g_s^2 C_F}{2} \int \frac{\mathbf{d}^4 k}{(2\pi)^4} \langle J/\psi | \bar{c} A_1^\alpha(l) b | B_c \rangle \frac{g_{\alpha\beta}}{l^2} \int \mathbf{d}z \frac{\mathbf{d}^2 \vec{k}_\perp}{16\pi^3} \frac{\Psi_\pi(z, \vec{k}_\perp)}{\sqrt{2N_c}} \mathbf{Tr} \left[\gamma_5 \not{A} A_2^\beta(l, k_d, k_{\bar{u}}) \right] \quad (26)$$

where l is the momentum of the internal gluon propagator, and

$$A_1^\alpha(l) = \gamma^\alpha \frac{\not{p}_c - \not{l} + m_c}{(p_c - l)^2 - m_c^2} \Gamma + \Gamma \frac{\not{p}_b + \not{l} + m_b}{(p_b + l)^2 - m_b^2} \gamma^\alpha \quad (27)$$

$$A_2^\beta(l, k_d, k_{\bar{u}}) = \Gamma \frac{\not{k}_{\bar{u}} + \not{l}}{(k_{\bar{u}} + l)^2} \gamma^\beta - \gamma^\beta \frac{\not{k}_d + \not{l}}{(k_d + l)^2} \Gamma \quad (28)$$

Here $\Gamma = \gamma_\mu(1-\gamma_5)$; p_b and p_c are the momentum of the b quark and the c quark, respectively. In fact, the terms in Eq.(26) are calculated using Feynman gauge. For an arbitrary covariant gauge, the internal gluon propagator should be written as [43]

$$\frac{-i}{l^2} \left(g_{\alpha\beta} + \eta \frac{l_\alpha l_\beta}{l^2} \right) \quad (29)$$

where $\eta = 0$ is the Feynman gauge, $\eta = -1$ is the Landau gauge.

Assuming that the external states are all physical and can be approximated as on-shell quarks in the leading order of Λ_{QCD}/m_b , it is easy to verify that for arbitrary covariant gauge, the terms proportional to η in Eq.(26) have no contribution, i.e. the expression of Eq.(26) is gauge independent. For instance,

$$\begin{aligned} l_\alpha l_\beta A_1^\alpha(l) &= l_\beta \not{l} \frac{\not{p}_c - \not{l} + m_c}{(p_c - l)^2 - m_c^2} \Gamma + \Gamma \frac{\not{p}_b + \not{l} + m_b}{(p_b + l)^2 - m_b^2} \not{l} l_\beta \\ &= -l_\beta \frac{2p_c \cdot l - l^2}{2p_c \cdot l - l^2} \Gamma + \Gamma \frac{2p_b \cdot l + l^2}{2p_b \cdot l + l^2} l_\beta = 0 \end{aligned} \quad (30)$$

Hence the gauge dependence cancels out when adding the two terms in A_1 . We can treat the A_2 in the similar way and get the result, $l_\alpha l_\beta A_2^\beta = 0$. More precisely, we find that the expression of Eq.(26) is gauge independent.

III. NUMERICAL RESULTS AND DISCUSSIONS

The expressions of decay amplitudes for $B_c \rightarrow J/\psi\pi$, $\eta_c\pi$ within the QCDF framework can be written as

$$\mathcal{A}(B_c^- \rightarrow J/\psi\pi^-) = \sqrt{2} G_F V_{cb} V_{ud}^* f_\pi A_0^{B_c \rightarrow J/\psi} m_{J/\psi} (\epsilon_{J/\psi} \cdot p_\pi) a_1 \quad (31)$$

$$\mathcal{A}(B_c^- \rightarrow \eta_c\pi^-) = -i \frac{G_F}{\sqrt{2}} V_{cb} V_{ud}^* f_\pi F_0^{B_c \rightarrow \eta_c} (m_{B_c}^2 - m_{\eta_c}^2) a_1 \quad (32)$$

The branching ratios in B_c meson rest frame can be written as:

$$BR(B_c \rightarrow X_{c\bar{c}}\pi) = \frac{\tau_{B_c}}{8\pi} \frac{|p|}{m_{B_c}^2} |\mathcal{A}(B_c \rightarrow X_{c\bar{c}}\pi)|^2 \quad (33)$$

where $X_{c\bar{c}}$ denotes J/ψ (or η_c) for $B_c \rightarrow J/\psi\pi$ (or $\eta_c\pi$) decays, and the momentum $|p| = (m_{B_c}^2 - m_{X_{c\bar{c}}}^2)/(2m_{B_c})$. The lifetime and mass for B_c meson are [3]: $m_{B_c} = 6.286 \pm 0.005$ GeV, and $\tau_{B_c} = 0.46_{-0.16}^{+0.18}$ ps.

To perform numerical calculations, we specify the input parameters as follows.

Nonperturbative hadronic quantities, such as meson decay constants, transition form factors, and meson distribution amplitudes, appear as inputs. In principle, information about these hadronic quantities can be obtained from experiments and/or estimated theoretically by non-perturbative method, such as lattice calculations, QCD sum rules, etc. In this paper, we shall follow the notation of [41] on hadron transition form factors. As a good approximation in the heavy quark limit, we shall take their values at the maximal recoil point for discussion. From the values collected in Table.II, we can see that there exists large uncertainty on theoretical predictions for $F_0^{B_c \rightarrow \eta_c}$ and $A_0^{B_c \rightarrow J/\psi}$. To estimate the branching ratios for $B_c \rightarrow J/\psi\pi$, $\eta_c\pi$ decays, we would like to take $F_0^{B_c \rightarrow \eta_c} = A_0^{B_c \rightarrow J/\psi} = 0.6$. We shall use the asymptotic form of the pion in the calculation, i.e. $\phi_\pi(z) = 6z\bar{z}$.

The Wolfenstein parameterization for the CKM matrix elements is used due to its advantage in explicitly expressing the hierarchy among the CKM elements in terms of powers of small parameter λ . With this notation, up to the order of $\mathcal{O}(\lambda^4)$, the CKM elements involved are $V_{cb} = A\lambda^2$, and $V_{ud} = 1 - \lambda^2/2$. The independent parameters of A and λ have been well determined to the accuracy of 1% and 0.1%, respectively. Their values are [3]

$$A = 0.818_{-0.017}^{+0.007}, \quad \lambda = 0.2272 \pm 0.0001 \quad (34)$$

Note that the relative weak phase difference is zero at this approximation, so no CP -violating asymmetry is expected.

Other input parameters are

$$\begin{aligned} m_u = m_d = m_s &= 0, & m_c &= 1.25 \pm 0.09 \text{ GeV [3]} \\ m_b &= 4.20 \pm 0.07 \text{ GeV [3]} & f_\pi &= 130.7 \pm 0.1 \pm 0.36 \text{ MeV [3]} \\ m_{J/\psi} &= 3096.916 \pm 0.011 \text{ MeV [3]} & m_{\eta_c} &= 2980.4 \pm 1.2 \text{ MeV [3]} \end{aligned}$$

If not specified explicitly, we shall take their central values as the default input.

Our numerical results are listed in Table I and III.

From the numbers in Table I, we can see that part information of strong phases is obtained by considering gluon radiative corrections to vertexes. Compared with the real part, the imaginary part of a_1 is small for $B_c \rightarrow J/\psi\pi$, $\eta_c\pi$. The reason is that the “nonfactorizable” effects are α_s or Λ_{QCD}/m_b suppressed within QCDF. Although the imaginary part is small, it will be very important for the exploration of CP violation for decay modes receiving contributions from both tree and penguin topologies. In fact, the numerical results of [32,

33, 42] indicate that the imaginary parts of most a_i ($i = 3, \dots, 10$) are the same order as the real parts, i.e. the “nonfactorizable” effects cannot be neglected for penguin-dominated decay modes.

It should be noted that both the imaginary part arising at the order of α_s and the real part of a_1 depend on the renormalization scale. But the scale dependence of a_1 has been reduced compared with that of NF, at least at the order of α_s . This can be seen from the Eq.(25) and Fig.2. In principle, high order of α_s corrections could be calculated order by order. Perhaps the remaining scale dependence of a_1 could be cancelled by the contributions from higher order of α_s corrections.

The numerical results of the branching ratios for $B_c \rightarrow J/\psi\pi$, $\eta_c\pi$ decays are given in Table III. From the numbers in Table III, we can see that these two branching ratios are close to each other, if we assume $A_0^{B_c \rightarrow J/\psi} = F_0^{B_c \rightarrow \eta_c}$. In fact, this point can also be seen from their relationship

$$\frac{\mathcal{BR}(B_c \rightarrow J/\psi\pi)}{\mathcal{BR}(B_c \rightarrow \eta_c\pi)} \simeq \frac{|A_0^{B_c \rightarrow J/\psi}|^2 (m_{B_c}^2 - m_{J/\psi}^2)^3}{|F_0^{B_c \rightarrow \eta_c}|^2 (m_{B_c}^2 - m_{\eta_c}^2)^3} \quad (35)$$

Some nonperturbative effects could be cancelled in the ratio of branching fraction. Using experimental data, the relation between the form factor $A_0^{B_c \rightarrow J/\psi}$ and $F_0^{B_c \rightarrow \eta_c}$ is expected to be obtained from the ratio Eq.(35). Once the nonperturbative parameters $A_0^{B_c \rightarrow J/\psi}$ and $F_0^{B_c \rightarrow \eta_c}$ are fixed, we might get some information on CKM element V_{cb} from Eq.(31) and Eq.(32).

In addition, from Table III we also see that the charm quark mass effect on the branching ratios is small, and that uncertainties from renormalization scale is also small. The uncertainties from the CKM elements which is proportional to $2\sigma_A/A$ are less than 5% [see Eq.(34)]. Thus the remaining uncertainties are the hadron parameters, such as transition form factors. Within QCDF approach, the transition form factor is the nonperturbative input parameter which comes from the long-distance contributions, so it must be computed nonperturbatively or determined experimentally. From the numbers in Table II, we can see that there are large differences in the numerical values of transition form factors $A_0^{B_c \rightarrow J/\psi}$, $F_0^{B_c \rightarrow \eta_c}$ for various theoretical approaches. So at the scale of $\mu = m_b$, the branching ratio can be rewritten as

$$\mathcal{BR}(B_c \rightarrow J/\psi\pi) = 0.119\% \times \frac{|A_0^{B_c \rightarrow J/\psi}|^2}{0.36} \quad (36)$$

$$\mathcal{BR}(B_c \rightarrow \eta_c \pi) = 0.128\% \times \frac{|F_0^{B_c \rightarrow \eta_c}|^2}{0.36} \quad (37)$$

The effects of transition form factors on the branching ratios are displayed in Fig.3 ^a, including the uncertainties from the CKM elements, quark masses and the renormalization scale. (Here the uncertainties from Λ_{QCD}/m_b corrections is not included, but it is assumed that its contribution is power suppressed and should not be large [32]) Clearly, the largest theoretical uncertainty comes from the transition form factors, which is of a nonperturbative nature within the QCD framework. Here we can not compute these form factors within QCD factorization scheme. We just use them as input parameters.

IV. SUMMARY AND CONCLUSION

In this paper, we calculated the hadronic matrix element for $b \rightarrow c$ transition at one-loop level under NDR scheme and in the heavy quark limit. Then we apply the master QCD formula to the would-be well detectable decay channels in experiments $B_c \rightarrow J/\psi\pi$, $\eta_c\pi$. The “nonfactorizable” vertex corrections are computed. We find that in the heavy quark limit, the “nonfactorizable” contributions dominated by hard gluon exchange can compensate the renormalization scale-dependence of the Wilson coefficients and are infrared safe and gauge independent. Finally, we give the branching ratios for $B_c \rightarrow J/\psi\pi$, $\eta_c\pi$ decays using the asymptotic distribution amplitude of the pion. We find that the large theoretical uncertainties come mainly from the non-perturbative transition form factors.

Acknowledgments

This work is Supported in part both by National Natural Science Foundation of China under Grant No. 10647119, 10710146, 10375041, 90403024 and by Natural Science Foundation of Henan Province, China (Grant No. 2008B140006). We would like to thank Prof.

^a Here, we think that theoretical prediction on nonperturbative parameters, such as transition form factors, relies on hard-to-quantify educated guesswork, due to our present inability to compute precisely strong interactions at long distances. All values within allowed ranges should be treated on an equal footing, irrespective of how close they are from the edges of the allowed range. So we had better to give a range in Fig.3 to show the theoretical uncertainties, rather than the form of Eq.(34).

Yadong Yang and Dr. Shuxian Du for valuable discussions.

- [1] F. Abe, *et al.* (CDF Collaboration), Phys. Rev. **D58**, 112004, (1998); Phys. Rev. Lett. **81**, 2432, (1998).
- [2] N. Cabibbo, Phys. Rev. Lett. **10**, 531, (1963); M. Kobayashi, and T. Maskawa, Prog. Theor. Phys. **49**, 652, (1973).
- [3] W. M. Yao, *et al.*, J. Phys. G: Nucl. Part. Phys. **33**, 1, (2006). (URL: <http://pdg.lbl.gov>)
- [4] D. Du, Z. Wang, Phys. Rev. **D39**, 1342, (1989).
- [5] M. Lusignoli, M. Masetti, Z. Phys. **C51**, 549, (1991).
- [6] P. Colangelo, G. Nardulli, N. Paver, Z. Phys. **C57**, 43, (1993).
- [7] C. H. Chang, Y. Q. Chen, Phys. Rev. **D49**, 3399, (1994).
- [8] J. F. Lu, K. T. Chao, Phys. Rev. **D56**, 4133, (1997).
- [9] A. Abd El-Hady, J. H. Muñoz, J. P. Vary, Phys. Rev. **D62**, 014019, (2000).
- [10] V. V. Kiselev, A. E. Kovalsky, A. K. Likhoded, Nucl. Phys. **B585**, 353, (2000).
- [11] V. A. Saleev, Phys. of Atomic Nuclei **64**, 2027, (2001).
- [12] V. V. Kiselev, O. N. Pakhomova, V. A. Saleev, J. Phys. G: Nucl. Part. Phys. **28**, 595, (2002).
- [13] V. V. Kiselev, J. Phys. G: Nucl. Part. Phys. **30**, 1445, (2004).
- [14] D. Ebert, R. N. Faustov, V. O. Galkin, Phys. Rev. **D68**, 094020, (2003); Eur. Phys. J. **C32**, 29, (2003).
- [15] M. A. Ivanov, J. G. Körner, O. N. Pakhomova, Phys. Lett. **B555**, 189, (2003).
- [16] M. A. Ivanov, J. G. Körner, P. Santorelli, Phys. Rev. **D73**, 054024, (2006).
- [17] C. H. Chang, Int. J. Mod. Phys. **A21**, 777, (2006).
- [18] W. Wang, Y. L. Shen, C. D. Lü, arXiv:0704.2493 [hep-ph].
- [19] N. Brambilla, *et al.*, hep-ph/0412158.
- [20] A. Abulencia, *et al.* (CDF Collaboration), Phys. Rev. Lett. **96**, 082002, (2006); Phys. Rev. Lett. **97**, 012002, (2006).
- [21] M. Beneke, G. Buchalla, M. Neubert and C. T. Sachrajda, Phys. Rev. Lett. **83**, 1914, (1999); Nucl. Phys. **B591**, 313, (2000).
- [22] C. H. Chang, and H. N. Li, Phys. Rev. **D55**, 5577, (1997).
- [23] T. W. Yeh, and H. N. Li, Phys. Rev. **D56**, 1615, (1997).

- [24] Y. Y. Keum, H. N. Li, and A. I. Sanda, Phys. Lett. **B504**, 6, (2001); Phys. Rev. **D63**, 054008, (2001).
- [25] C. W. Bauer, S. Fleming, D. Pirjol, I. W. Stewart, Phys. Rev. **D63**, 114020, (2001).
- [26] C. W. Bauer, D. Pirjol, I. W. Stewart, Phys. Rev. **D65**, 054022, (2002).
- [27] A. Ali, G. Kramer, and C. D. Lü, Phys. Rev. **D58**, 094009, (1998); Phys. Rev. **D59**, 014005, (1998).
- [28] Y. H. Chen, H. Y. Cheng, and B. Tseng, Phys. Rev. **D59**, 074003, (1999).
- [29] Y. H. Chen, H. Y. Cheng, B. Tseng, and K. C. Yang, Phys. Rev. **D60**, 094014, (1999).
- [30] H. Y. Cheng, and K. C. Yang, Phys. Lett. **B511**, 40, (2001).
- [31] D. S. Du, D. S. Yang, and G. H. Zhu, Phys. Lett. **B488**, 46, (2000).
- [32] M. Beneke, G. Buchalla, M. Neubert, and C. T. Sachrajda, Nucl. Phys. **B606**, 245, (2001).
- [33] D. S. Du, H. J. Gong, J. F. Sun, D. S. Yang, and G. H. Zhu, Phys. Rev. **D65**, 074001, (2002); Phys. Rev. **D65**, 094025, (2002); and Erratum, *ibid.* **D66**, 079904, (2002);
- [34] J. F. Sun, G. H. Zhu, D. S. Du, Phys. Rev. **D68**, 054003, (2003).
- [35] M. Beneke, M. Neubert, Nucl. Phys. **B675**, 333, (2003).
- [36] W. J. Zou, Z. J. Xiao, Phys. Rev. **D72**, 094026, (2005);
Z. J. Xiao, W. J. Zou, Phys. Rev. **D70**, 094008, (2004).
- [37] M. Beneke, Phys. Lett. **B620**, 143, (2005).
- [38] M. Beneke, J. Rohrer, D. S. Yang, Nucl. Phys. **B774**, 64, (2007).
- [39] A. Ali, G. Kramer, Y. Li, C. D. Lü, Y. L. Shen, W. Wang, Y. M. Wang, Eur. Phys. J. **C51**, 841, (2007).
- [40] For a review, see G. Buchalla, A. J. Buras and M. E. Lautenbacher, Rev. Mod. Phys. **68**, 1125, (1996); or A. J. Buras, hep-ph/9806471.
- [41] M. Wirbel, B. Stech, and M. Bauer, Z. Phys. **C29**, 637, (1985); M. Bauer, B. Stech, and M. Wirbel, Z. Phys. **C34**, 103, (1987).
- [42] D. S. Du, D. S. Yang, and G. H. Zhu, Phys. Lett. **B509**, 263, (2001); Phys. Rev. **D64**, 014036, (2001).
- [43] R. D. Field, *Applications of Perturbative QCD*, 1989, Addison-Wesley Publishing Company, Inc.
- [44] V. V. Kiselev, A. Tkabladze, Phys. Rev. **D48**, 5208, (1993)
- [45] V. V. Kiselev, A. K. Likhoded, A. I. Onishchenko, Nucl. Phys. **B569**, 473, (2000)

[46] M. A. Ivanov, J. G. Kömer, P. Santorelli, Phys. Rev. **D63**, 074010, (2001)

[47] T. Huang, F. Zuo, hep-ph/0702147.

[48] M. A. Ivanov, J. G. Kömer, P. Santorelli, Phys. Rev. **D71**, 094006, (2005)

TABLE I: Wilson coefficients C_i and a_1 in the NDR scheme.

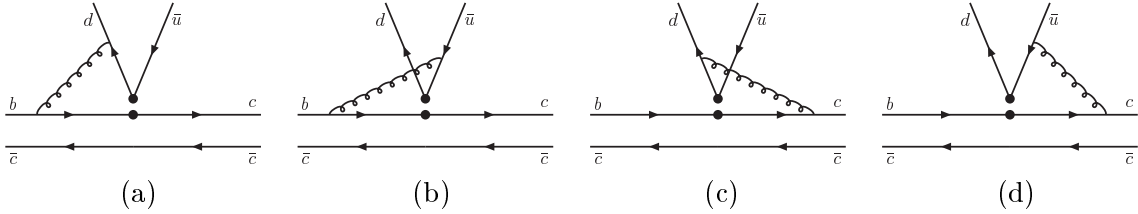
μ (GeV)	NLO		LO		NF	QCDF	
	C_1	C_2	C_1	C_2	a_1	a_1 ($m_c = 1.25$ GeV)	a_1 ($m_c = 0$)
2.0	1.147	-0.304	1.191	-0.374	1.046	$1.084 + i0.034$	$1.079 + i0.036$
3.0	1.109	-0.236	1.148	-0.303	1.031	$1.070 + i0.024$	$1.066 + i0.025$
4.0	1.088	-0.196	1.124	-0.261	1.023	$1.061 + i0.019$	$1.058 + i0.020$
5.0	1.074	-0.169	1.108	-0.232	1.018	$1.054 + i0.016$	$1.052 + i0.016$
6.0	1.064	-0.148	1.096	-0.210	1.014	$1.049 + i0.013$	$1.047 + i0.014$
7.0	1.056	-0.131	1.087	-0.192	1.012	$1.045 + i0.012$	$1.043 + i0.012$
8.0	1.049	-0.118	1.079	-0.178	1.010	$1.041 + i0.011$	$1.040 + i0.011$

TABLE II: Values of transition form factors

Reference	$F_0^{B_c \rightarrow \eta_c}$	$A_0^{B_c \rightarrow J/\psi}$
[4]	0.170 ~ 0.687	0.156 ~ 0.684
[6]	0.20 ± 0.02	0.26 ± 0.07^a
[44]	0.23 ± 0.01	0.21 ± 0.03^b
[45]	0.66	0.595^c
[46]	0.76	0.69^d
[47]	0.87	0.27^e
[14]	0.47	0.40
[48]	0.61	0.57^f
[18]		$0.57^{+0.01}_{-0.02}$

TABLE III: Branching ratios for $B_c \rightarrow J/\psi\pi, \eta_c\pi$ (in the unit of %).

μ	$\mathcal{BR}(B_c \rightarrow J/\psi\pi)$			$\mathcal{BR}(B_c \rightarrow \eta_c\pi)$		
	NF	QCDF	QCDF	NF	QCDF	QCDF
		$(m_c = 0)$	$(m_c = 1.25 \text{ GeV})$		$(m_c = 0)$	$(m_c = 1.25 \text{ GeV})$
$m_b/2$	0.116	0.123	0.124	0.124	0.132	0.134
m_b	0.111	0.119	0.119	0.119	0.127	0.128
$2m_b$	0.108	0.114	0.115	0.116	0.123	0.123


 FIG. 1: Vertex corrections to hard-scattering kernel for $b \rightarrow c$ decay at the order of α_s . The upward lines represent the valence quarks of the emitted π meson.

^a Compared the definitions of transition form factor of Ref.[41] with those of Ref.[6], we can obtain their relationships at the maximal recoil point,

$$A_0^{B_c \rightarrow J/\psi} = \frac{F_0^A}{2m_{J/\psi}} + \frac{m_{B_c}^2 - m_{J/\psi}^2}{2m_{J/\psi}} F_+^A \quad (38)$$

where the transition form factor $A_0^{B_c \rightarrow J/\psi}$ is defined in [41], F_0^A and F_+^A are defined in [6], and their values are $F_0^A = 2.5 \pm 0.3 \text{ GeV}^{-1}$, $F_+^A = -0.03 \pm 0.01 \text{ GeV}^{-1}$.

^b Using the relationship of Eq.(38) and the values of $F_0^A = 2.0 \pm 0.2 \text{ GeV}^{-1}$, $F_+^A = -0.024 \pm 0.002 \text{ GeV}^{-1}$ [44]

^c Using the relationship of Eq.(38) and the values of $F_0^A = 5.9 \text{ GeV}^{-1}$, $F_+^A = -0.074 \text{ GeV}^{-1}$ [44]

^d Compared the definitions of transition form factor of Ref.[41] with those of Ref.[46], we can obtain their relationships at the maximal recoil point,

$$A_0^{B_c \rightarrow J/\psi} = \frac{m_{B_c} + m_{J/\psi}}{2m_{J/\psi}} A_1 - \frac{m_{B_c} - m_{J/\psi}}{2m_{J/\psi}} A_2 \quad (39)$$

where A_1 and A_2 are defined in [46], and their values are $A_1 = 0.68$, $A_2 = 0.66$.

^e Using the relationship of Eq.(39) and the values of $A_1 = 0.75$, $A_2 = 1.69$. [47]

^f Compared the definitions of transition form factor of Ref.[41] with those of Ref.[48], we can obtain their relationships at the maximal recoil point,

$$A_0^{B_c \rightarrow J/\psi} = \frac{m_{B_c} - m_{J/\psi}}{2m_{J/\psi}} (A_0 - A_+) \quad (40)$$

where A_0 and A_+ are defined in [48], and their values are $A_0 = 1.64$, $A_+ = 0.54$.

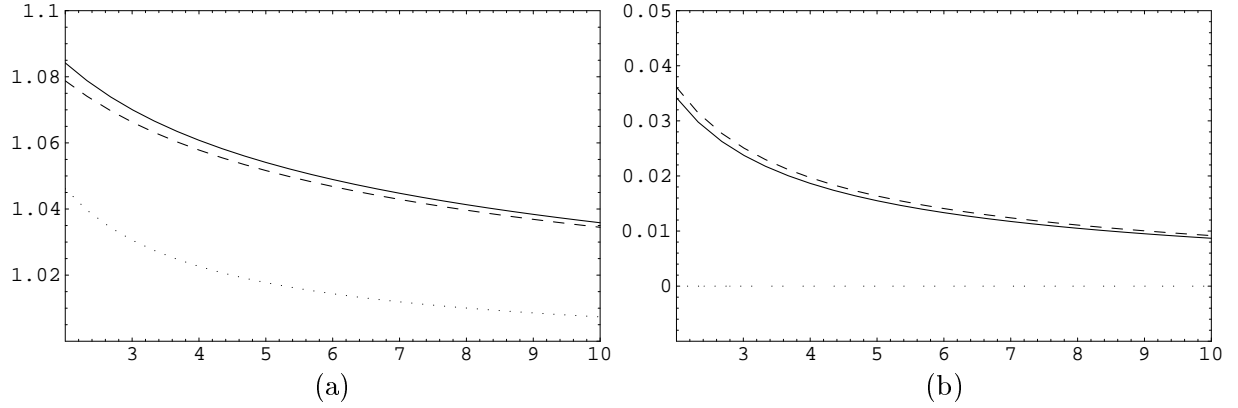


FIG. 2: Dependence of the coefficient a_1 [vertical axes, $\text{Re}(a_1)$ in (a) and $\text{Im}(a_1)$ in (b)] on the renormalization scale μ [horizontal axes, in units of GeV], with asymptotic light-cone distribution amplitudes $\phi_\pi(x) = 6x\bar{x}$. The solid and dashed lines denote a_1 for the case of $m_c = 1.25$ GeV and $m_c = 0$ within QCDF framework, respectively; the dotted line denotes a_1 within NF framework.

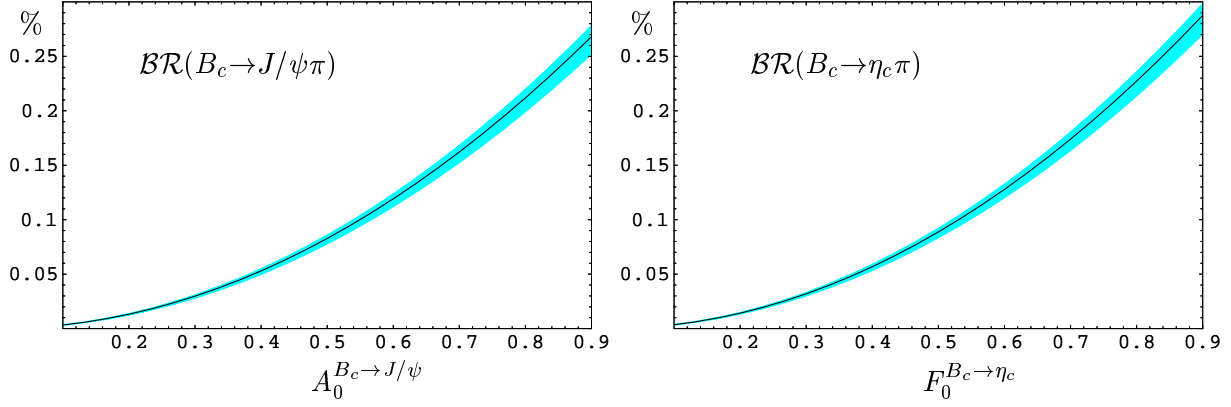


FIG. 3: Branching ratios for $B_c \rightarrow J/\psi\pi$, $\eta_c\pi$ versus the transition form factors $A_0^{B_c \rightarrow J/\psi}$, $F_0^{B_c \rightarrow \eta_c}$ in the QCDF approach, considering the mass of c quark. The solid lines are calculated with central values of inputs, while the bands denote the uncertainties from CKM elements and quark masses.